2D mapping of plane stress crack-tip fields following an overload

P. J. Withers
School of Materials, Grosvenor St, University of Manchester, Manchester M13 9PL, UK and The Research Complex at Harwell, Rutherford Appleton Laboratory, Didcot, Oxfordshire OX11 0FA, UK
philip.withers@manchester.ac.uk

P. Lopez-Crespo
Department of Civil and Materials Engineering, University of Malaga, C/ Doctor Ortiz Ramos, s/n, 29071, Malaga, Spain
plopezcrespo@uma.es

M. Mostafavi
Department of Mechanical Engineering, University of Sheffield, Sir Frederick Mappin Building, Mappin Street, Sheffield S1 3JD, UK
m.mostafavi@sheffield.ac.uk

A. Steuwer
Nelson Mandela Metropolitan University, Gardham Av., 6031 Port Elizabeth, South Africa
axel.steuwer@gmail.com

J. F. Kelleher
ISIS, Science and Technology Facilities Council, Rutherford Appleton Laboratory, Didcot, Oxfordshire OX11 0QX, UK
joe.kelleher@stfc.ac.uk

T. Buslaps
ESRF, 6 rue J Horowitz, 38000, Grenoble, France
buslaps@esrf.fr

ABSTRACT. The evolution of crack-tip strain fields in a thin (plane stress) compact tension sample following an overload (OL) event has been studied using two different experimental techniques. Surface behaviour has been characterised by Digital Image Correlation (DIC), while the bulk behaviour has been characterised by means of synchrotron X-ray diffraction (XRD). The combination of both surface and bulk information allowed us to visualise the through-thickness evolution of the strain fields before the OL event, during the overload event, just after OL and at various stages after it. Unlike previous work, complete 2D maps of strains around the crack-tip were acquired at 60μm spatial resolution by XRD. The DIC shows less crack opening after overload and the XRD a lower crack-tip peak stress after OL until the crack has grown past the compressive crack-tip residual stress introduced by the overload after which the behaviour returned to that for the baseline fatigue response. While the peak crack-tip stress is supressed by the compressive residual stress, the crack-tip stress field changes over each cycle are nevertheless the same for all K_{max} cycles except at OL.

KEYWORDS. Linear elastic fracture mechanics; Closure; Plastic strain; Bainitic steel; Effective stress intensity factor.

INTRODUCTION

Many crack retardation effects occurring during the fatigue of materials have been explained by the concept of crack closure [1]. Closure of the crack-faces either near to, or distant from, the crack-tip means that the crack-tip does not experience the full crack-opening fatigue cycle. Such effects have been held to be responsible for the immediate acceleration and then subsequent retardation of the crack growth rate observed following an overload during fatigue cycling.

Diffraction peak shifts are predominantly sensitive to the elastic strain and a number of studies have mapped the strain ahead of, and behind, the crack-tip using neutron [2, 3] or synchrotron x-ray [4, 5] beams. The problem with linescans along the crack plane is that there is a danger that the location of the peak stress may be missed. Steuwer et al. [6] were the first to map the stresses in thick (plane strain) samples in 2D at high (25μm) resolution, but in this case the plastic zone was small and the crack-tip stress fields dominated largely by elastic behaviour.

In this paper, we employ Digital Image Correlation (DIC), a non-contact full-field measurement technique, to measure the total (elastic plus plastic) strain on the surface of the specimen. The accuracy of DIC to measure elastic strain is debateable, but its capability to measure total strain (considering that plastic strains are orders of magnitude bigger than elastic strains) is unrivalled. The combination of the two techniques provides both elastic (from XRD) and total (DIC) strains if the measurements are carried out on the same gauge volume. Therefore, we selected a thin (i.e. plane stress) specimen so that the variation of the strain field on the surface, where DIC measures the total strain, and the elastic strain averaged through thickness as measured by XRD, is minimised. DIC has found increasing application for the study of crack-tip strain fields [7] and it has been possible to extract fracture mechanics information such as closure stresses [8, 9], plastic zone sizes [10], crack-tip opening displacements (CTOD) and effective stress intensity factors at the crack-tip, K^{eff} [10-14].

Lopez-Crespo et al. have already combined these complementary methods to examine the strain fields local to a crack-tip in a plane stress (thin) stainless steel compact tension sample prior and subsequent to an overload event [15]. Even under plane stress where the surface and bulk states might be expected to be the same, important differences were observed between DIC and XRD. Surface DIC measurements suggested that under fatigue cycling the cracks faces appear to be in contact for around 50% of the cycle supporting a traditional plasticity-induced closure interpretation. Indeed they observed a knee in the closure response for baseline fatigue prior to overload, an absence of closure in the accelerated growth regime followed by accentuated closure in the retardation regime. By contrast, measurement of the mid-thickness elastic strain field behind and ahead of the crack made by synchrotron X-ray diffraction showed no evidence of significant crack-face contact stresses immediately behind the crack-tip on approaching minimum loading. Though the results were affected by point-to-point scatter due to an insufficiently small grain size, the changes during loading and overloading could mostly be explained by a simple elastic plastic analysis using a value of the yield stress intermediate between the initial yield stress and the UTS. This showed very significant compressive plastic strains ahead of the crack that start to form early during unloading.

Here we revisit this topic by studying a bainitic rather than stainless steel. This has an inherently much finer grain size allowing us to achieve much higher spatial resolution in the X-ray diffraction data with much reduced point to point scatter [16]. Further the steel has sufficient toughness that a large plastic zone can be introduced in contrast to the Al-Li studied by Steuwer et al. [6]. This has enabled us to study the elastic strain field and the effect of plasticity on closure in unparalleled detail.

MATERIAL AND SPECIMEN

A compact tension (CT) fatigue specimen was machined from quenched and tempered bainitic steel similar to Q1N (HY80) [17]. Its chemical composition is summarised in Tab. 1. The tensile properties are as follows: Yield Stress (σ_y) = 570 MPa and Ultimate Tensile Stress, σ_{uts}= 663 MPa. The CT specimen had a width (W) of 60 mm and thickness (B) of 3.3mm.

Alloy	C	Si	Mn	P	S	Cr	Ni	Mo	Cu
Q1N	0.16	0.25	0.31	0.010	0.008	1.42	2.71	0.41	0.10

Table 1: Chemical composition in weight % of Q1N steel. The balance is Fe.

EXPERIMENTAL SETUP

The crack-tip elastic strain fields were measured on the ID15 beamline at the European Synchrotron Radiation Facility (ESRF), using the same arrangement as that described in [6] and shown schematically in Fig. 1a. The incident beam slits were opened to 60×60 μm giving a lateral resolution (x,y) of 60 μm and a nominal gauge length through-thickness (z) of around 1.4 mm (diamond shaped centred on the mid-plane ($z=0$)). This allowed a 10 times greater resolution than in previous elastic strain field mapping experiments for plastically extended crack-tips [15]. Such a good resolution was possible because of the small grain size of the bainitic steel used here.
The DIC was undertaken simultaneously using a single camera set-up [9] taking contrast from the speckle paint as shown in Fig 1. The slightly oblique view of the sample was corrected for before the analysis of the data. Commercial DIC analysis software (La Vision GmbH, Gottingen, Germany) was used to analyse the results and details of the approach are provided in [18].
In this experiment great care was taken to correct for the slight sample movements that took place when the sample was fatigued and when it was statically loaded to K_{max} (=35 MPa√m) and K_{min} (=1.2 MPa√m) to ensure that all of the strain maps were recorded with respect to the sample coordinates and not the lab coordinates. To this end both shifts recorded by DIC analysis and by edge scans by XRD were used. It is estimated that we were able to correct the sample location to ±50 μm.

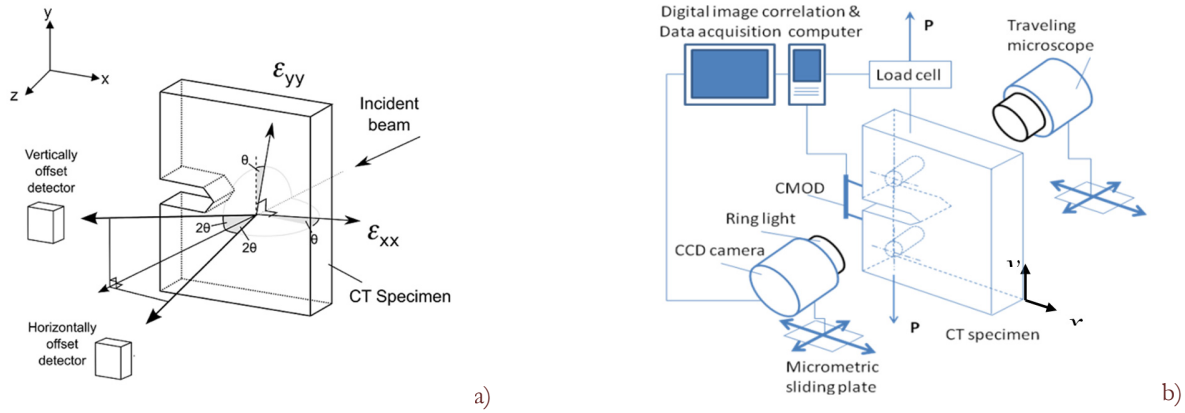

Figure 1: Schematics showing a) the diffraction geometry with two detectors so as to measure two in-plane directions of strain; note the coordinate system for ε_{xx} and ε_{yy}. For very low θ, these strains can be taken as representative of those in the loading (y) and crack growth (x) directions, b) the DIC arrangement [9]. In actual fact the camera viewed the sample at a slight angle to allow the X-ray beam unimpeded access to the sample.

FATIGUE EXPERIMENT

The specimen was fatigue pre-cracked for 3000 cycles at a frequency of 10 Hz, stress intensity range $\Delta K=35$ MPa√m and load ratio $K_{min}/K_{max}=0.03$. Plane stress conditions were met at the mid-plane through the thickness for all loads applied during the experiment [19]. The crack length was measured perpendicularly to the loading direction from the centre of the loading holes [20]. Once the fatigue crack had grown to a length of 12.75 mm, a 67% overload (OL) was applied. Strain measurements were made at a number of fatigue stages, namely during the cycle just before the overload (OL-1), during the overload (OL), 40 cycles after the overload (OL+40), 2040 cycles after the overload (OL+2k), 8040 cycles after the overload (OL+8k) and 37540 cycles after the overload (OL+37k). In addition to

2D maps, a profile of the evolution of strain behind and ahead of the crack-tip was produced for each of the fatigue stages studied by measuring around 50 strain points along the crack plane (y=0) at different distances from the location of the crack at overload. Crack growth in the specimen was measured from the overload location using XRD line scans: 0.08mm for OL+40, 0.22mm for OL+2k, 0.27mm for OL+8k and 2.05mm for OL+37k cycles. These values were used for correcting the current location of the crack tip at each loading stage in the following results.

RESULTS AND DISCUSSION

The elastic strains were measured directly from the diffraction profiles using a Rietveld-style refinement to obtain the lattice spacing representative of the diffraction peaks as a whole. Elastic strain maps were obtained showing very little point-to-point scatter. The elastic strains parallel to the loading direction (ε_{yy}) and parallel to the crack growth direction (ε_{xx}) are shown in Fig. 2 at the overload. The elastic strain fields are broadly similar in shape and magnitude to those recorded by Steuwer et al. [6]. The images taken from the surface of the sample were analysed using LaVision Davis v6.4 employing a least square algorithm with subset size 31 (patch size) and step size 8 pixels (75% overlap).

The corresponding total (elastic plus plastic) strains recorded at $1.7K_{max}$ were obtained from DIC and are also shown in Fig 2. Unsurprisingly, the elastic strains are 5-10 times smaller than the total strains local to the crack due to plastic deformation. A simple Irwin analysis would predict a plastic zone of around 3.5 mm for the overload event (60MPa√m). The DIC shows clearly the characteristic plastic lobes.

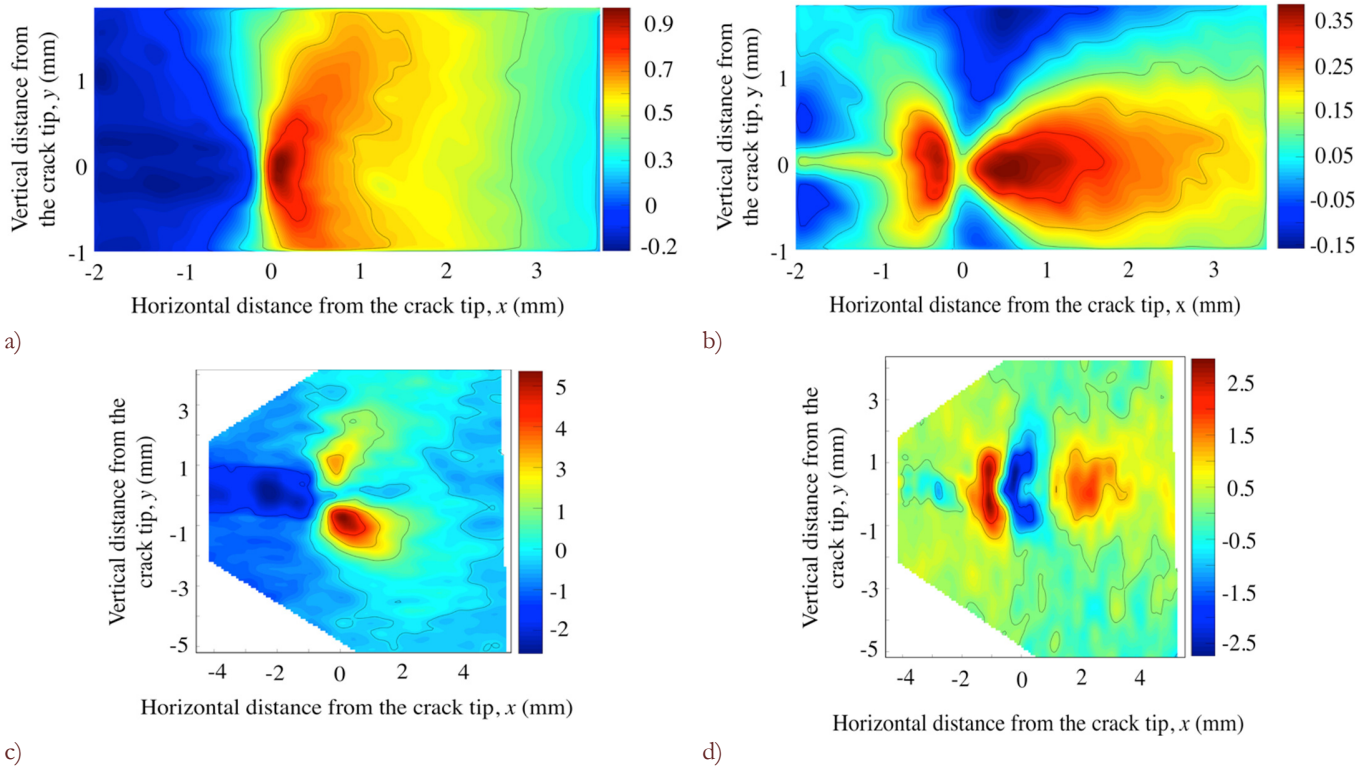

Figure 2: Strain maps at overload (OL) showing the elastic strains measured by XRD in the a) loading direction ε_{yy} (%) and b) parallel to the crack growth direction ε_{xx} (%) and the total strain measured by DIC in the c) loading direction ε^{tot}_{yy} (%) and d) parallel the crack growth direction ε^{tot}_{xx} (%). The XRD measurements were performed while the sample was loaded at the maximum load ($1.7K_{max}$); the DIC strains were calculated from full-field displacements measured by comparing the images of the surface of the sample taken at maximum load ($1.7K_{max}$) and minimum load (K_{min}) in the cycle just before the overload.

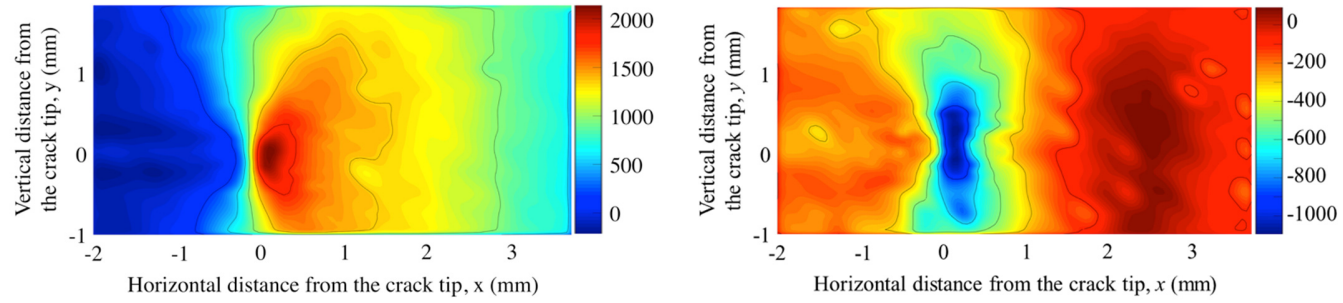

a) b)

Figure 3: Mid-plane maps of stress in the loading direction σ_{yy} (in MPa) calculated from the elastic ε_{xx} and ε_{yy} measured by synchrotron XRD a) at OL ($1.7K_{max}$) b) immediately after OL at minimum load (K_{min}). Note the different colours scales used.

Unfortunately it is not possible to measure the through-thickness elastic strain ε_{zz} with the same spatial definition as the two in-plane strains, however the stresses can be inferred using the relation for plane stress ($\sigma_{zz} = 0$) using the diffraction elastic constants representative of the polycrystal because all the diffraction peaks were used in the refinement.

$$\sigma_{xx} = \frac{E}{1-\nu^2}\left[\varepsilon_{xx} + \nu\varepsilon_{yy}\right]$$

The crack-tip stress in the loading direction is shown in Fig. 3a), which clearly shows the classical butterfly stress field (HRR field) formed around the crack-tip. The 2D elastic stress field within the plastic zone has not been mapped in previous studies. The DIC data allow the crack opening displacement to be mapped in the vicinity of the crack (Fig. 4a). It is clear from the DIC (Fig. 2) that the plastic zone extends 3-4mm ahead of the crack tip although its magnitude falls away quickly. The residual stress field shows a slight tensile hump around 2.5mm ahead of the crack (see later discussion).

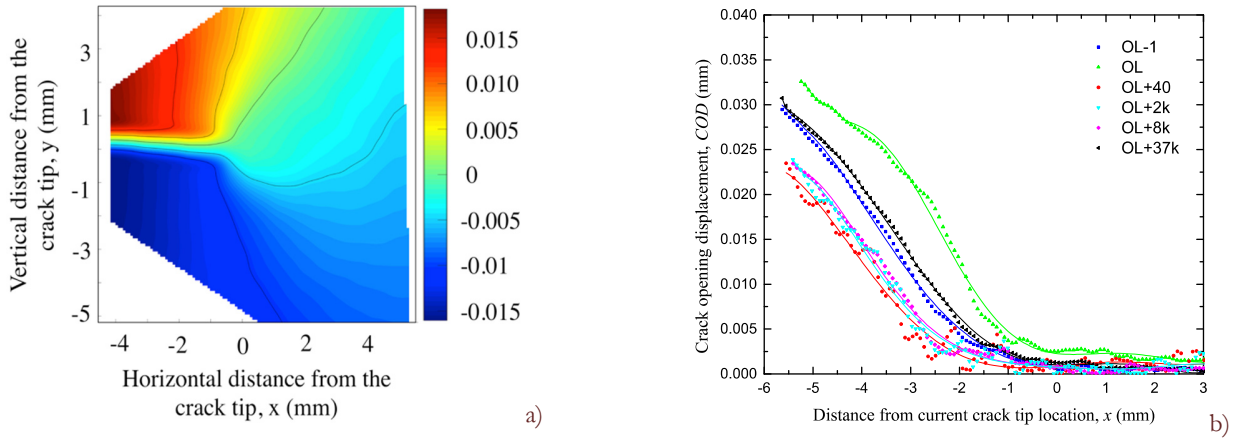

a) b)

Figure 4: DIC analysis showing the a) vertical displacement field V_y (in mm) between $1.7K_{max}$ (OL) and at K_{min} prior to OL, b) change in crack opening displacement (ΔCOD) profiles at maximum load using the state at K_{min} prior to OL as the reference state.

The effect of the compressive residual stress field, which has been generated at the crack-tip by the overload, on the peak stress in the loading direction after (OL+40) compared with that measured before the (OL-1) overload is evident in Fig. 5a. An approximately 50% decrease is observed in the maximum stress in the crack loading direction near the crack-tip before and after the overload. The magnitude of the residual stress induced by the overload can be estimated by comparing the peak compressive stress just ahead of the crack-tip before and after the overload (see Fig. 5b). As can be seen in the figure the maximum compressive stress at K_{min} just before the overload is approximately 550MPa which increases to almost 1000MPa immediately after the overload. It is clear from Fig. 5c that the elastic change in stress in the crack-tip region upon loading to K_{max} is essentially the same as that for the baseline fatigue cycle (OL-1) for all the post overload cycles, it is just that post OL the cycles are displaced by the compressive residual stress field introduced by the OL event. This is consistent with the observations of Lopez-Crespo et al. [16] for a thick (plane strain) CT sample of the same steel.

The change in crack opening displacement (ΔCOD) between minimum and maximum load with distance behind the crack tip is shown in Fig. 4b. Unsurprisingly the crack opening is much greater at OL than prior to it (OL-1). After OL the crack opening displacement appears to be reduced (by around 30%) at K_{max} relative to OL-1 for the first 8k cycles returning to a level similar to that for OL-1 after 37k cycles. The reduction in the change in crack opening (i.e. crack opening displacement between first K_{min} before OL and K_{max} at each loading state) displacement can be interpreted as 54% reduction in the effective stress intensity factor range and is consistent with plasticity-induced crack closure. Given the resolution of the DIC system, the crack can be assumed to be closed if COD < 2.5 μm. Accordingly, the crack length can be fictitiously reduced by 1mm for OL-1 and OL+37k and by 2mm for OL+40, OL+2k and OL+8k. This may be because of the closure effects, which might be expected to be most prominent on the surface where the DIC measurements are made and does not allow the crack to open beyond the resolution of the DIC and therefore gives the impression of a shorter crack.

There are a number of other interesting features relating to the stress profiles shown in Fig. 5. Most importantly, it is evident that only when the crack has grown through the compressive residual stress field introduced by the OL, does the COD or the peak crack-tip elastic strain field revert to that representative of the original baseline fatigue response (OL-1). Secondly, the 'hump' in the stress in the crack-opening direction which is generated 2.5mm ahead of the crack when the overload is applied is retained for the OL+40, +2k and +8k cycles but is not present for the baseline fatigue or for the last increment. Because the unload curves are elastic the 'hump' is also evident in the unloaded profiles too. Both these observations are almost certainly connected to the fact that only after 37k cycles has the crack-tip grown sufficiently (by 2.05mm) to have emerged from the plastic zone introduced by the overload.

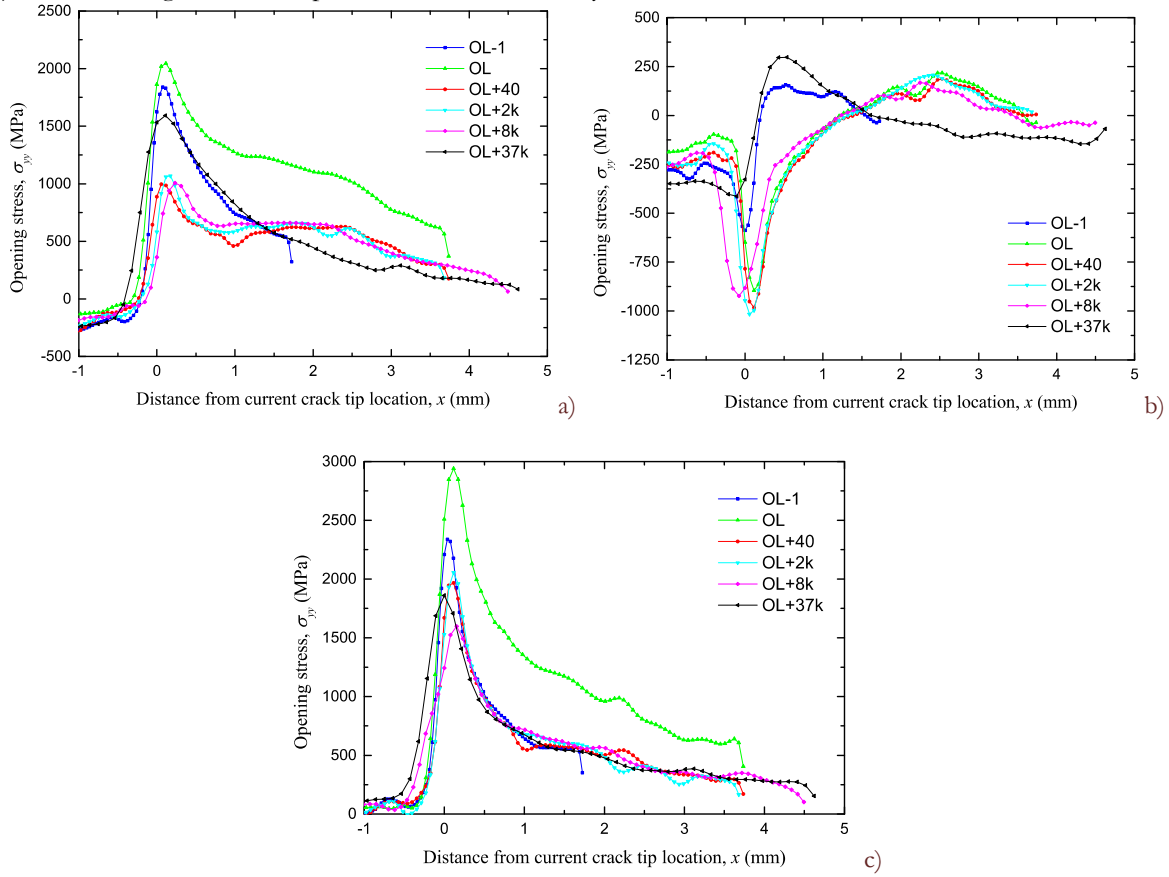

Figure 5: XRD line profiles along y=0 showing the crack loading stress σ_{yy} (MPa) a) at maximum load b) at minimum load and c) the difference between the stresses at maximum and minimum load at each stage in the fatigue crack growth response.

CONCLUSIONS

- X-ray diffraction and digital image correlation techniques were simultaneously used to successfully measure the change in the elastic and plastic strain fields around a fatigue crack after an overload

- The DIC surface strain measurements are consistent with a plastic zone extending some 3-4 mm ahead of the crack-tip; while the stresses recorded by diffraction show a slight tensile hump 2.5 mm ahead of the crack-tip.
- Both the elastic strain field measured by XRD and the crack opening displacement measured by DIC showed a reduction in their peak values as a result of the compressive residual stress field induced around the crack-tip after the overload
- Once the crack had grown through the sufficiently to have essentially both the change in crack opening displacement and the peak tensile crack-tip stress field returned to levels similar to that prior to the overload event.

ACKNOWLEDGEMENTS

The authors are grateful to the ESRF for ID15 beam-time awarded under MA1483.

REFERENCES

[1] Elber, W., Fatigue crack closure under cyclic tension, Eng. Fract. Mech., 2 (1970) 37-45.
[2] Hutchings, M.T., Hippsley, C.A., Rainey, V., Neutron Diffraction Measurement of the Stress Field During Fatigue Cycling of a Cracked Test Specimen, Mat. Res. Soc. Symp. Proc., 166 (1990) 317.
[3] Lee, S.Y., Liaw, P.K., Choo, H., Rogge, R.B., A study on fatigue crack growth behavior subjected to a single tensile overload Part I. An overload-induced transient crack growth micromechanism, Acta Materialia, 59 (2011) 485-494.
[4] Steuwer, A., Santisteban, J.R., Turski, M., Withers, P.J., Buslaps, T., High-resolution strain mapping in bulk samples using full-profile analysis of energy dispersive synchrotron X-ray diffraction data, Nucl. Instr. Meth. Physics Research B, 238B (2005) 200-204.
[5] Croft, M., Zhong, Z., Jisrawi, N., Zakharchenko, I., Holtz, R.L., Skaritka, J., Fast, T., Sadananda, K., Lakshmipathy, M., Tsakalakos, T., Strain profiling of fatigue crack overload effects using energy dispersive X-ray diffraction, International Journal of Fatigue, 27 (2005) 1408-1419.
[6] Steuwer, A., Rahman, M., Shterenlikht, A., Fitzpatrick, M.E., Edwards, L., Withers, P.J., The evolution of crack-tip stresses during a fatigue overload event, Acta. Mater., 58 (2010) 4039-4052.
[7] Sutton, M.A., McNeill, S.R., Helm, J.D., Boone, M.L., Measurement of crack tip opening displacement and full-field deformations during fracture of aerospace materials using 2D and 3D image correlation methods, Iutam Symposium on Advanced Optical Methods and Applications in Solid Mechanics, 82 (2000) 571-580.
[8] Nowell, D., de Matos, P.F.P., Application of digital image correlation to the investigation of crack closure following overloads, in: P. Lukas (Ed.) Fatigue 2010, (2010) 1035-1043.
[9] Yusof, F., Lopez-Crespo, P. P.J. Withers, Effect of overload on crack closure in thick and thin specimens via digital image correlation, International Journal of Fatigue, 56 (2013) 17-24.
[10] Lopez-Crespo, P., Shterenlikht, A., Yates, J.R., Patterson, E.A., Withers, P.J., Some experimental observations on crack closure and crack-tip plasticity, Fat. Fract. Eng. Mater, Struct., 32 (2009) 418-429
[11] Shterenlikht, A., Garrido, F.A.D., Crespo, P.L., Withers, P.J., Patterson, E.A., Mixed mode (K_I + K_{II}) stress intensity factor measurement with ESPI and image correlation, Adv. in Exp. Mech., 1-2 (2004) 107-112.
[12] Shterenlikht, A., Lopez-Crespo, P., Patterson, E.A., Withers, P.J., Yates, J.R., Determining stress and stress intensity from displacement fields using Muskhelishvili's approach, I. J. Fatigue, (2007).
[13] Lopez-Crespo, P., Shterenlikht, A., Patterson, E.A., Yates, J.R., Withers, P.J., The stress intensity of mixed mode cracks determined by digital image correlation J. Strain Anal. by Eng. Design, 43 (2008) 769-780.
[14] López-Crespo, P., Patterson, E.A., Shterenlikht, A., Withers, P.J., Yates, J.R., Study of a crack at a fastener hole by image correlation, Exp. Mech., 49 (2009) 551-559.
[15] Lopez-Crespo, P., Withers, P.J., Yusof, F., Dai, H., Steuwer, A., Kelleher, J.F., Buslaps, T., Overload effects on fatigue crack-tip fields under plane stress conditions: surface and bulk analysis, Fatigue and Fracture of Engineering Materials and Structures, 36 (2013) 75-84.
[16] Lopez-Crespo, P., Steuwer, A., Buslaps, T., Tai, Y.H., Lopez-Moreno, A., Yates, J.R., Withers, P.J., Measuring overload effects during fatigue crack growth in bainitic steel by synchrotron X-ray diffraction, International Journal of Fatigue, 71 (2015) 11-16.

[17] Robertson, I.M., Measurement of the effects of stress ratio and changes of stress ratio on fatigue crack growth rate in a quenched and tempered steel. , Int. J. Fatigue, 16 (1994) 216-220.
[18] Quinta da Fonseca, J., Mummery, P.M., Withers, P.J., Full-field strain mapping by optical correlation of micrographs acquired during deformation, J. Micros., 218 (2005) 9-21.
[19] Anderson, T.L., Fracture Mechanics, Fundamentals and Applications, 3rd Edition ed., CRC Press, (2005).
[20] Murakami, Y., Stress Intensity Factors Handbook, Oxford: Pergamon Press, (1987).